



Saitoh, K., Varshney, S., Sasaki, K., Rosa, L., Pal, M., Paul, MC., Ghosh, D., Bhadra, SK. & Koshiba, M. (2011). Limitation on effective area of bent large-mode-area leakage channel fibers.

Originally published in *Journal of Lightwave Technology*, 29(17), 2609-2615.  
Available from: <http://dx.doi.org/10.1109/jlt.2011.2161603>

Copyright © 2011 IEEE.

This is the author's version of the work. It is posted here with the permission of the publisher for your personal use. No further distribution is permitted. If your library has a subscription to this journal, you may also be able to access the published version via the library catalogue.



# Limitation on Effective Area of Bent Large-Mode-Area Leakage Channel Fibers

Kunimasa Saitoh, *Member, IEEE, Member, OSA*, Shailendra Varshney, *Member, IEEE, Member, OSA*, Kaori Sasaki, Lorenzo Rosa, *Member, IEEE*, Mrinmay Pal, Mukul Paul, Debashri Ghosh, Shyamal Bhadra, and Masanori Koshiba, *Fellow, IEEE, Fellow, OSA*

**Abstract**— We investigate the bending characteristics of leakage channel fibers (LCFs) to achieve large-mode-area (LMA) and effectively single-mode operation with a practically allowable bending radius for compact Yb-doped fiber applications. Through numerical simulations, carried by the full-vectorial finite element method, we present the limitations on the effective area of LCFs under bent condition and compare their limits with that of conventional step-index LMA fibers. Due to a better controllability of the low numerical aperture and a large value of the differential bending loss ( $\sim 20$  dB/m) between the fundamental and higher-order modes in LCFs, the LMA of  $\sim 500 \mu\text{m}^2$  (core diameter of  $\sim 36 \mu\text{m}$ ) at 1064 nm can be achieved when the optimized LCF is bent into a 10 cm bending radius.

**Index Terms**— Effectively single-mode, fiber lasers, large mode area fibers, leakage channel fibers, microstructured optical fibers.

## I. INTRODUCTION

IN recent years, there has been a growing interest in achieving a large mode area (LMA) fiber designs for laser applications [1]–[5]. However most of the fiber designs are limited by the bending losses (BLs) for compact packaging [6]. LMA can be achieved either by increasing the core diameter or by decreasing the numerical aperture (NA) of the fiber. However, to maintain single-mode operation, the relative refractive index difference between core and cladding should be decreased as the core diameter is increased, resulting in a large BL. This issue can be overcome through the deployment of specially-designed optical fibers with higher NA that can achieve an effectively single-mode (ESM) operation regime by limiting the propagation of the higher-order modes (HOMs). However, in the conventional fiber technology, the increment of the core size is limited by the difficulty of precise control of

the index profile when NA is very low. Another way to achieve LMA fibers is to employ resonant structures [7], however, their refractive index profiles are complicated and an accurate control of the index profile is required, resulting in fabrication issues and high fabrication cost.

To overcome these issues, various types of microstructured optical fibers (MOFs) have been investigated so far [8], [9], which can provide low NA without a germanium doped core. The presence of air-holes or low-index inclusions (e.g. fluorine-doped silica rods) in the cladding induces a strong wavelength dependence of the cladding index that gives an additional degree of freedom to control the NA, which can be tuned by changing the size of the low-index elements, making it possible to achieve a core diameter  $>100 \mu\text{m}$  with single-mode operation [10]. However, it should be noticed that such MOFs with very large core diameter are not suitable for Yb-doped fiber amplification in coiled condition with a practical bending radius as low as 5 cm to 10 cm [11], as the effective mode area shrinks too much. One of the promising and simple ways to achieve LMA fibers with ESM condition and relatively low BL is to employ leakage channel fibers (LCFs) [12]–[18], characterized by a cladding formed by a single air-hole ring or a few of them. In this case, however, the limitation of the core size enlargement with bending has not been investigated in detail under practical constraints. Under bent conditions the fiber propagation characteristics change so that a reduction in the effective area may cause the onset of nonlinear processes in the fiber, deteriorating the output power and energy storage capacity [6], [19]. Therefore, it becomes necessary to formulate criteria to maintain a stable mode-field shape along with LMA in a standard packaging environment.

In this paper, we investigate bending characteristics of LCFs to achieve LMA and ESM operation with a practically allowable bending radius of  $R= 5$  cm to 10 cm at 1064-nm wavelength for Yb-doped fiber applications and discuss their superiority over conventional step-index LMA fibers having low multimodality. Through detailed numerical simulations based on the finite element method (FEM) [20], [21], we found that the LCFs having two rings of low-index inclusions (air or fluorine-doped silica rods) can introduce sufficient differential BL between the fundamental mode (FM) and the HOMs, and push the effective area limit to much larger values with respect to conventional LMA step-index fibers (SIFs).

Manuscript received May 11, 2011.

K. Saitoh, K. Sasaki, and M. Koshiba are with the Graduate School of Information Science and Technology, Hokkaido University, Sapporo 060-0814, Japan (phone: +81-11-706-6542; fax: +81-11-706-7892; e-mail: ksaitoh@ist.hokudai.ac.jp).

S. Varshney is with the Department of E&ECE, Indian Institute of Technology, Kharagpur-721302, India.

L. Rosa is with the Centre for Micro-Photonics, Swinburne University of Technology, Hawthorn, VIC 3122, Australia.

M. Pal, M. Paul, D. Ghosh, and S. Bhadra are with the Fibre Optics Division, Central Glass & Ceramic Research Institute, Kolkata - 700032, India.

Color version of one or more of the figures in this paper are available online at <http://ieeexplore.ieee.org>.

Digital Object Identifier ?

II. EFFECTIVE AREA LIMIT IN STEP-INDEX LMA FIBERS UNDER BENT CONDITION

We consider the core size limits in conventional SIFs, as shown in Fig. 1(a), in bending condition. In designing LMA fibers, we target packaging radii of 5 cm to 10 cm and a large differential BL between the FM and the HOM to maintain single-mode propagation at the 1064 nm operating wavelength. The upper and lower BL limits of the FM and the HOMs are set to 0.1 dB/m and 10 dB/m, respectively, to obtain and optimize suitable fiber parameters. These criteria are reasonable in general, since the fiber length using for amplifier or laser is about 5 to 10 meters in the most practical applications.

Figures 1(b), (c), and (d) show the variation of effective area at 1064 nm in SIFs with bending radii of 5 cm, 7.5 cm, and 10 cm, respectively, calculated by the FEM. The core diameter varies from 20  $\mu\text{m}$  to 35  $\mu\text{m}$  and the relative refractive index difference between the core index  $n_{\text{core}}$  and the cladding index  $n_{\text{clad}}$  is defined as  $\Delta_{\text{core}} = (n_{\text{core}}^2 - n_{\text{clad}}^2) / (2n_{\text{core}}^2)$ , where the background material is assumed to be silica with refractive index of  $n_{\text{clad}} = 1.45$ . The solid red and blue curves indicate a BL value of 0.1 dB/m (FM) and 10 dB/m (LP<sub>11</sub>-like HOM), respectively. The HOM condition of  $\text{BL}_{\text{HOM}} > 10$  dB/m is satisfied below the blue curve, whereas the FM condition of  $\text{BL}_{\text{FM}} < 0.1$  dB/m is satisfied above the red curve. From this graph, we find that an ESM effective area larger than 500  $\mu\text{m}^2$  is achievable for 10 cm bending radius, if we can maintain a low refractive index difference value  $\Delta_{\text{core}}$ . However, we have to note that it is rather difficult to achieve a very low NA < 0.06 ( $\Delta_{\text{core}} < 0.085\%$ ) in SIFs due to practical issues in finely controlling such a small dopant concentration difference in the fabrication process. Therefore, we would need to tighten the bending radius to values  $\leq 5$  cm, as in Fig. 1(b), to obtain ESM operation with manageable  $\Delta_{\text{core}}$ , but this may result in a severe mode field distortion in the LMA fiber.

As we fix the minimum practical SIF NA=0.06, Fig. 2 shows the relationship between the core diameter and the required bending radius for achieving the ESM condition at 1064 nm. The red and blue curves are defined as before, and the upper limits of effective area ( $A_{\text{eff}}$ ) at the BL limits are also plotted. Taking into account the fabrication tolerance of the index profile and the bending radius tolerance with  $\pm 0.5$  cm errors, we can deduce a core diameter upper limit of  $\sim 27$   $\mu\text{m}$  and a corresponding effective area limit of approximately 350  $\mu\text{m}^2$  for the ESM SIF with bending radius smaller than 10 cm. This also suggests that the upper limit of the core size can be further increased if we can realize a lower NA (<0.06) while keeping a low FM BL. Due to the flexibility of MOFs, such novel fibers are able to overcome the SIF LMA limits in bent condition by carefully designing their structural parameters.

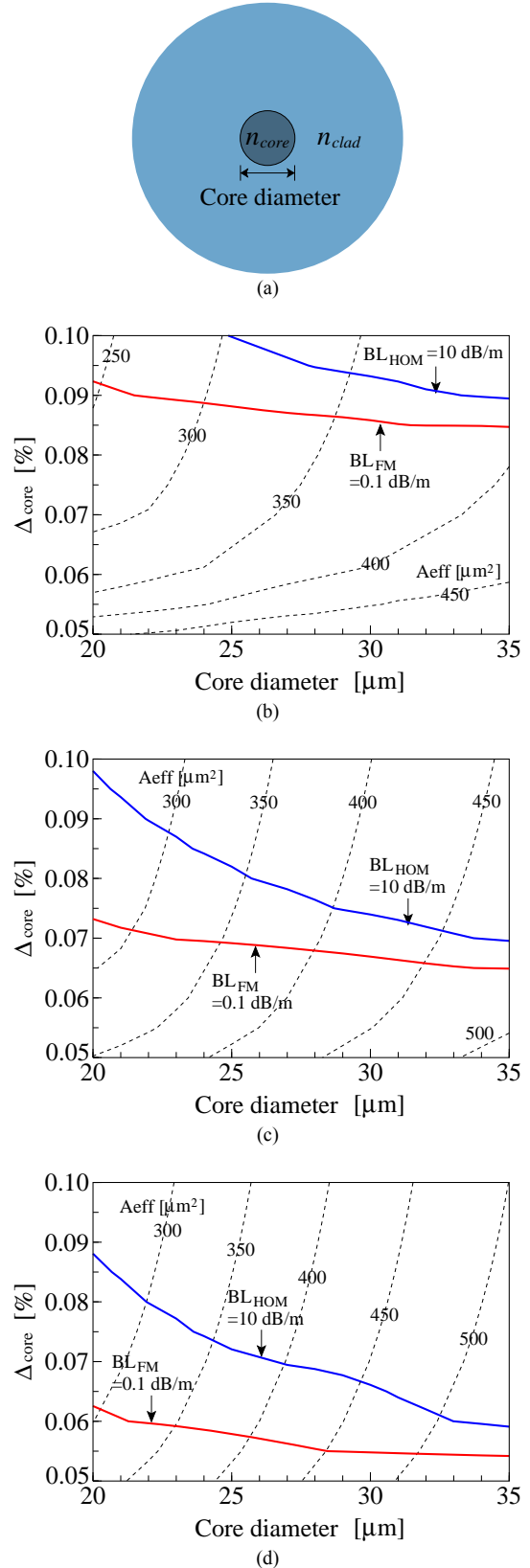


Fig. 1. (a) Schematic cross-section of an SIF and variation of effective area as a function of the core diameter and the relative refractive index difference  $\Delta_{\text{core}}$  in the SIF with bending radius of (b)  $R=5$  cm, (c)  $R=7.5$  cm, and (d)  $R=10$  cm. The solid red and blue curves correspond to the lower and upper limits of the bending loss of FM and HOM, respectively.

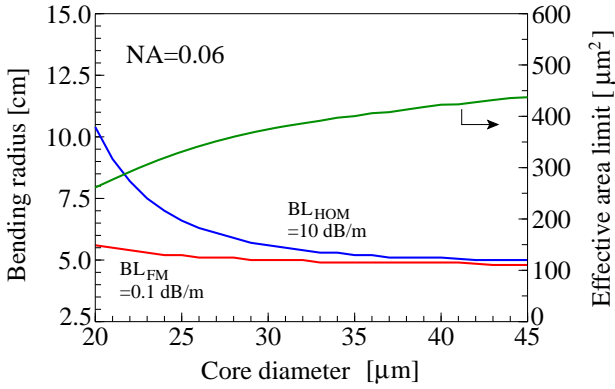


Fig. 2. Relationship between the core diameter and the required bending radius in SIFs with NA=0.06 for achieving ESM condition at 1064-nm wavelength. The red and blue curves correspond to the lower and upper limits of the bending loss of FM and HOM, respectively. The upper limits of effective area are also plotted.

### III. BENDING CHARACTERISTICS IN LEAKAGE CHANNEL FIBERS

A layout of the simplest LCF design is shown in Fig. 3(a), which is a LCF with one air-hole ring structure. The LCF is characterized by its geometrical parameters, air-hole diameter  $d$  and the spacing between the air-holes  $\Lambda$ . In designing the LMA LCF, we target a LMA condition for standard packaging radii of 5 cm-10 cm and a large differential BL between the FM and the HOM, to achieve ESM propagation at 1064 nm. The upper and lower BL limits of the FM and the HOMs are set similarly to the previously mentioned LMA SIF design. Usually, the differential loss between FM and HOM in LCFs is evaluated in the straight case. However here we evaluate it in the bent case as it is more relevant in practical situations. In addition, the core material is assumed to be pure silica for simplicity in our calculations. However, in the actual Yb-doped LCF with high doping concentration, the refractive index in the doped region would be slightly increased. This index increase can be lowered by co-doping of fluorine to tune the doping region index to pure silica level, therefore the following results are also valid for the Yb-doped LCFs.

Figures 3(b), (c), and (d) show the variation of effective area at 1064 nm in LCFs containing one air-hole ring for bending radii of 5 cm, 7.5 cm, and 10 cm, respectively. The air-hole pitch  $\Lambda$  is varied from 20 μm to 35 μm and the normalized air-hole size  $d/\Lambda$  is varied from 0.7 to 0.8, and the background material is assumed to be silica as before. Note that the material dispersion of silica has been ignored in the calculations. If we consider the wavelength-dependent silica index, it will only scale the results, but will not affect the results significantly. The solid red and blue curves are defined as in the SIF, where now the HOM is a LP<sub>11</sub>-like group formed by the TE<sub>01</sub> mode, the TM<sub>01</sub> mode, and the degenerated HE<sub>21</sub> modes. The HOM condition of BL<sub>HOM</sub> > 10 dB/m is satisfied below the blue curve, whereas the FM condition of BL<sub>FM</sub> < 0.1 dB/m is satisfied above the red curve. If we fix  $d/\Lambda$  and move  $\Lambda$  to a higher value, we will enlarge the core size with respect to wavelength.

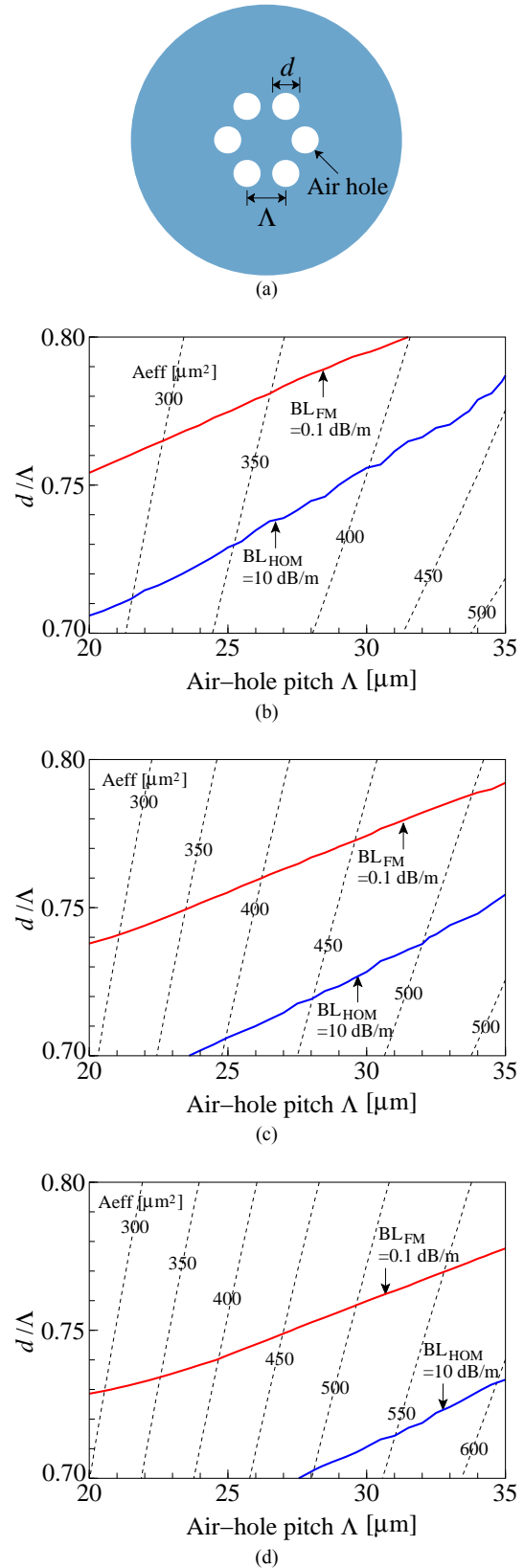


Fig. 3. (a) Schematic cross-section of an LCF with one air-hole ring structure and variation of effective area as a function of the air-hole pitch  $\Lambda$  and the normalized air-hole size  $d/\Lambda$  in the one-ring LCF with bending radius of (b)  $R=5$  cm, (b)  $R=7.5$  cm, and (c)  $R=10$  cm. The solid red and blue curves correspond to the lower and upper limits of the bending loss of FM and HOM, respectively.

However, in this situation, the bending loss increases due to the decrement of NA. Therefore, the upper limit of  $d/\Lambda$  for the HOM as well as the lower limit of  $d/\Lambda$  for the FM increase as increasing the pitch value. From these results, we can clearly observe that for a single ring LCF design, the solid red curve always stays above the blue curve. This means that a one-ring LCF can not satisfy simultaneously both constraints of low loss operation and ESM condition, because the bending loss of all modes decreases as the value of  $d/\Lambda$  increases. Therefore, the one-ring LCF structure (as shown in Fig. 3(a)) is not suitable to achieve ESM LMA behavior in bending condition, as it is not possible to achieve a sufficiently high differential BL.

Due to the impossibility of achieving LMA in the one-ring LCF while satisfying the targeted constraints, we consider a LCF design with a two air-hole ring structure, shown in Fig. 4(a), in order to increase the differential mode loss. The fiber design improves on the previous one by adding an additional ring that can further control the BL. Figures 4(b), (c), and (d) show the variation of effective area at 1064 nm in such LCFs for bending radii of 5 cm, 7.5 cm, and 10 cm, respectively. The air-hole pitch  $\Lambda$  varies from 20  $\mu\text{m}$  to 35  $\mu\text{m}$  and the normalized air-hole size  $d/\Lambda$  varies from 0.65 to 0.75, in pure silica glass as before. The HOM condition of  $BL_{\text{HOM}} > 10 \text{ dB/m}$  is satisfied below the blue curve, whereas the FM condition of  $BL_{\text{FM}} < 0.1 \text{ dB/m}$  is satisfied above the red curve. From these results, with the same curve color definitions, we deduce the existence of upper limits of the air-hole pitch (and corresponding core size limits) for each bending radius.

The crossing point between the red curve and blue curve represents the theoretical limit of the effective area, and thus the theoretical limits of air-hole pitch are 25  $\mu\text{m}$ , 28  $\mu\text{m}$ , and 31  $\mu\text{m}$  for the bending radii of 5 cm, 7.5 cm, and 10 cm, respectively, while the maximum value of the normalized air-hole size  $d/\Lambda$  ( $\sim 0.72$ ) is almost constant for each bending radius. However, note that it might be difficult to fabricate LCF structures having such precise values of the structural parameters with the required accuracy. Thus, from this analysis and from the knowledge of the fabrication process accuracy, we can estimate a practical upper limit of  $\sim 0.67$  for the normalized air-hole size  $d/\Lambda$ .

As we fix the maximum practical  $d/\Lambda=0.67$ , Fig. 5 shows the relationship between the air-hole pitch  $\Lambda$  and the required bending radius in two air-hole ring LCFs in ESM condition at 1064 nm, together with the upper limits of effective area ( $A_{\text{eff}}$ ). There is a reasonable bending radius tolerance for  $\Lambda > 24 \mu\text{m}$  and, based on this analysis, we can clearly set  $\sim 27 \mu\text{m}$  as the upper limit of air-hole pitch, which gives the corresponding effective area limit as approximately 500  $\mu\text{m}^2$  for bending radius  $< 10 \text{ cm}$  to achieve ESM operation.

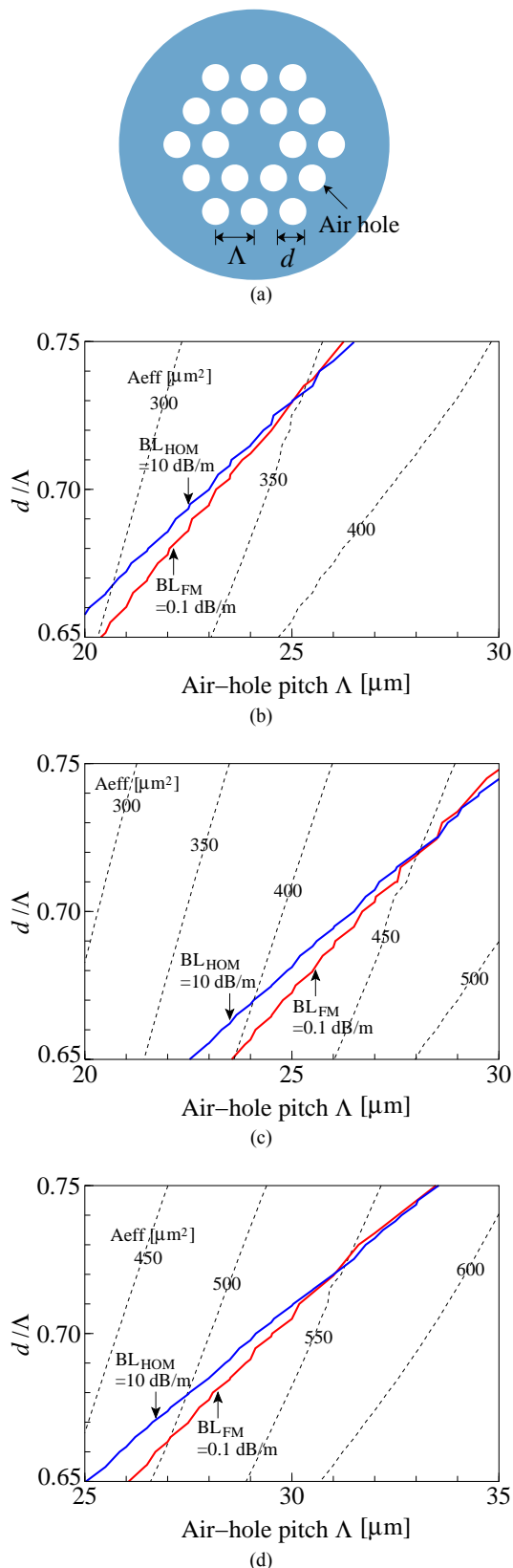


Fig. 4. (a) Schematic cross-section of an LCF with two air-hole ring structure and variation of effective area as a function of the air-hole pitch  $\Lambda$  and the normalized air-hole size  $d/\Lambda$  in the two-ring LCF with bending radius of (b)  $R=5 \text{ cm}$ , (c)  $R=7.5 \text{ cm}$ , and (d)  $R=10 \text{ cm}$ . The solid red and blue curves correspond to the lower and upper limits of the bending loss of FM and HOM, respectively.

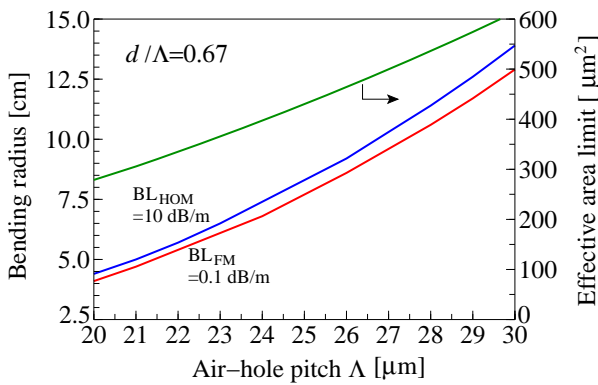


Fig. 5. Relationship between the air-hole pitch  $\Lambda$  and the required bending radius in two air-hole ring LCFs with  $d/\Lambda=0.67$  for achieving ESM condition at 1064-nm wavelength. The red and blue curves correspond to the lower and upper limits of the bending loss of FM and HOM, respectively. The upper limits of effective area are also plotted.

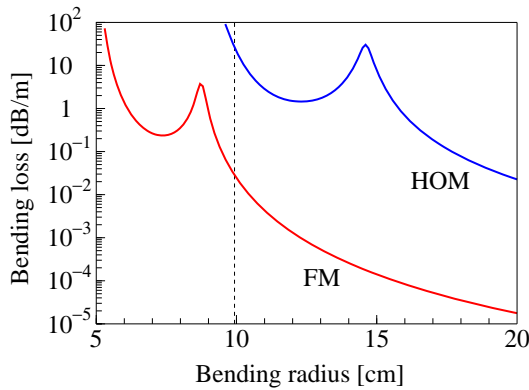


Fig. 6. Bending losses of the FM and the first HOM as a function of bending radius in a two-ring LCF at 1064 nm, where  $\Lambda=27 \mu\text{m}$ , and  $d/\Lambda=0.67$ .

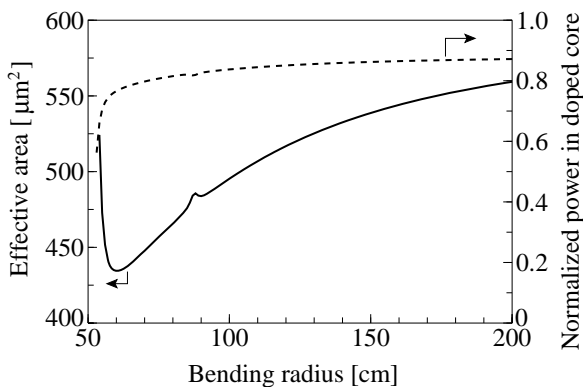


Fig. 7. Effective area variation and the normalized power in doped-core region of the FM as a function of bending radius in a two-ring LCF at 1064 nm, where  $\Lambda=27 \mu\text{m}$ ,  $d/\Lambda=0.67$ , and the doped-core diameter is assumed to be  $27 \mu\text{m}$ .

Figure 6 displays the BL in the two-ring LCF as a function of bending radius at 1064 nm, where  $\Lambda=27 \mu\text{m}$  and  $d/\Lambda=0.67$ . The red and blue curves represent the BLs of FM and HOM, respectively. The BL peaks, around bending radius of 8.6 cm for the FM and 14.6 cm for the HOM, are attributed to the coupling between the guided core mode and the cladding modes [22]. Except for the peaks, BL increases monotonically for

tighter bending. A high enough differential BL between the FM and the HOM can be found: the FM BL remains lower than 0.03 dB/m, whereas for the HOM it is larger than 20 dB/m at the same bending radius of 10 cm. In Fig. 7, the variation of the FM effective area as a function of the bending radius at 1064-nm wavelength is plotted. The effective area decreases monotonically with smaller bending and attains a value of  $495 \mu\text{m}^2$  at the bending radius of 10 cm, while it is equal to  $592 \mu\text{m}^2$  in the straight condition. The effective area compression due to bending is only 16 %. The mode field distributions at 1064 nm in the straight and bent cases are shown in Figs. 8(a) and (b), respectively, achieving a very good confinement of the FM and a reasonably low distortion due to bending, which does not substantially compromise the doped region overlap. In Fig. 7, we have also plotted the normalized power in doped-core region of the FM as a function of the bending radius at 1064-nm wavelength, where the circular doped-core region with core diameter of  $27 \mu\text{m}$  is assumed. We can see that the normalized power in the circular doped core is about 84 % at the bending radius of 10 cm.

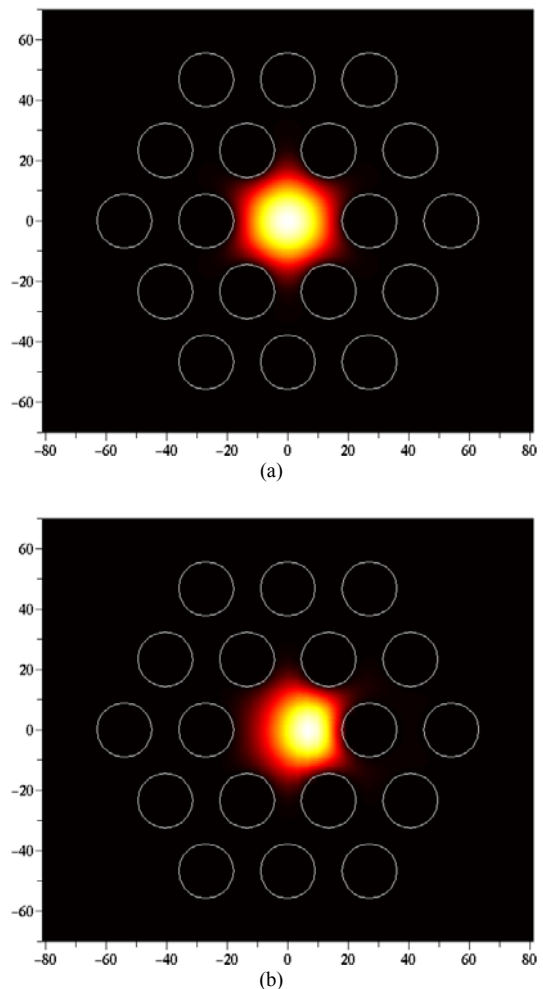


Fig. 8. Mode field distributions at 1064 nm in a two-ring LCF (a) without bending and (b) with bending radius of  $R=10 \text{ cm}$ , where  $\Lambda=27 \mu\text{m}$ , and  $d/\Lambda=0.67$ .

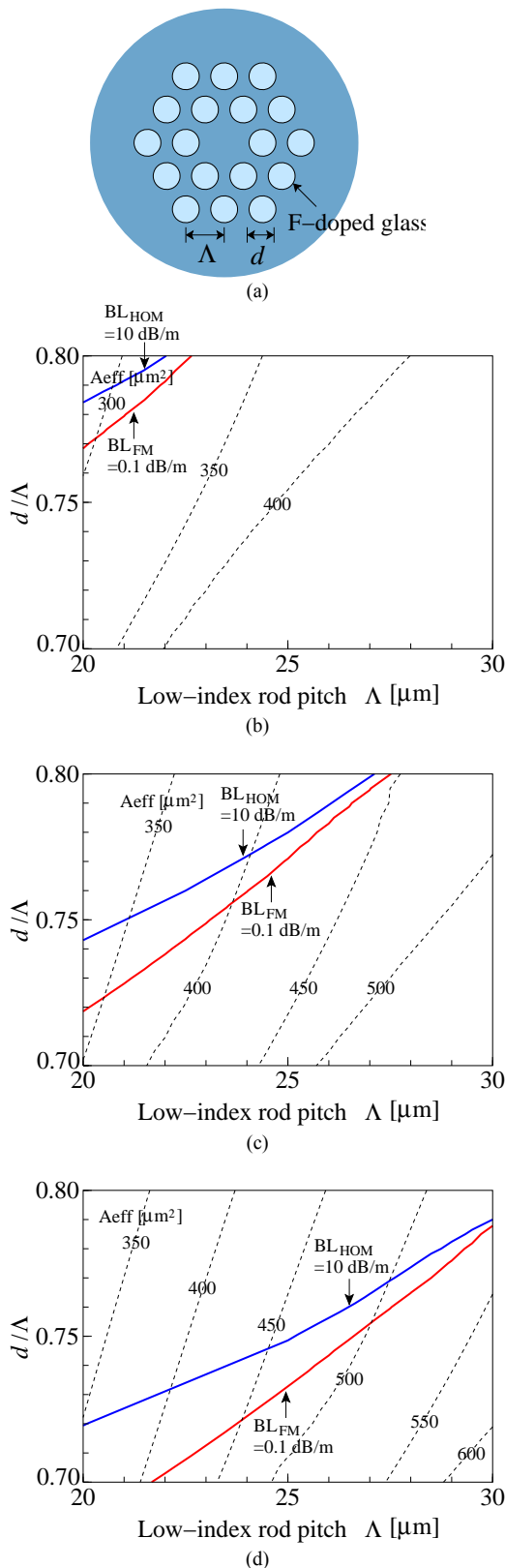


Fig. 9. (a) Schematic cross-section of an all-glass LCF with two rings of F-doped silica rods and variation of effective area as a function of the low-index rod pitch  $\Lambda$  and the normalized rod size  $d/\Lambda$  in the two-ring LCF with bending radius of (b)  $R=5$  cm, (c)  $R=7.5$  cm, and (d)  $R=10$  cm, where  $\Delta^- = 0.4\%$ . The solid red and blue curves correspond to the lower and upper limits of the

bending loss of FM and HOM, respectively.

Finally, we consider an all-glass LCF design, shown in Fig. 9(a), with the aim to further improve the NA and LMA characteristics. An LCF with an array of air-holes around the core requires to be sealed, and the resulting local refractive index perturbations can lead to mode distortion, having an even larger impact on the mode structure due to the large core size [12]. Therefore, to reduce mode distortion and achieve an easier LCF fabrication as well as low splice loss, an all-glass LCF design has been reported [12], in which the air-holes are replaced by fluorine-doped (F-doped) silica rods, whose refractive index is lower than that of pure silica. Figure 9(a) shows an all-glass LCF with two rings of F-doped silica rods. The F-doped silica rod diameter is  $d$  and the center-to-center rod spacing is  $\Lambda$ . The background material is pure silica and the relative refractive index difference between the two kinds of material is defined as  $\Delta^- = (n_{clad}^2 - n_F^2) / (2n_{clad}^2)$ , where  $n_{clad}$  is the index of pure silica and  $n_F$  is the index of F-doped silica. In the following calculations, we will assume  $\Delta^- = 0.4\%$  as an example.

Figures 9(b), (c), and (d) show the effective area at 1064 nm in all-glass LCFs with two F-doped silica rod rings for bending radii of 5 cm, 7.5 cm, and 10 cm, respectively. The rod pitch  $\Lambda$  varies from 20  $\mu\text{m}$  to 30  $\mu\text{m}$  and  $d/\Lambda$  varies from 0.7 to 0.8, embedded in pure silica. From these results, with the same curve color definitions, we can deduce the upper limit of core size for each bending radius. We find that the practical effective area limit in the all-glass LCFs is very similar to that in the two air-hole ring LCFs, which is around 500  $\mu\text{m}^2$  with bending radius of 10 cm. However, the main advantages of all-glass LCF would be the ease of fabrication and the reduced parameter tolerance levels.

#### IV. CONCLUSION

The practical limits of the effective area for effectively single-mode LMA fibers have been investigated for fiber laser/amplifier applications under bending conditions. The bending characteristics of LMA LCFs as well as SIFs are numerically evaluated and it is found that the upper limit of the effective area for the ESM operation with bending radius smaller than 10 cm is less than 350  $\mu\text{m}^2$  in a conventional SIF by considering the index profile controllability, while for the two-ring LCF structures it can be improved to around 500  $\mu\text{m}^2$  (core diameter of  $\sim 36$   $\mu\text{m}$ ) at 1064-nm wavelength with reasonable fabrication tolerances. We have also numerically confirmed that these effective area limits can not be improved even if we use lower or higher doping concentration of the F-doped glass.

#### REFERENCES

- [1] N.G.R. Broderick, H.L. Offerhaus, D.J. Richardson, R.A. Sammut, J. Caplen, and L. Dong, "Large mode area fibers for high power applications," *Opt. Fib. Technol.*, vol. 5, no. 2, pp. 185-196, Apr. 1999.
- [2] J.P. Koplow, D.A.V. Kliner, and L. Goldberg, "Single-mode operation of a coiled multimode fiber amplifier," *Opt. Lett.*, vol. 25, no. 7, pp. 442-444, Apr. 2000.

- [3] A. Galvanauskas, "Mode-scalable fiber-based chirped pulse amplification systems," *IEEE J. Sel. Top. Quantum Electron.*, vol. 7, no. 4, pp. 504-517, July/Aug. 2001.
- [4] Y. Jeong, J.K. Sahu, D.N. Payne, and J. Nilsson, "Ytterbium-doped large-core fibre laser with 1 kW of continuous-wave output power," *Electron. Lett.*, vol. 40, no. 8, pp. 470-472, Apr. 2004.
- [5] M.M. Vogel, M. Abdou-Ahmed, A. Voss, and T. Graf, "Very-large-mode-area, single-mode multicore fiber," *Opt. Lett.*, vol. 34, no. 18, pp. 2876-2878, Sept. 2009.
- [6] M.J. Li, X. Chen, A. Liu, S. Gray, J. Wang, D. T. Walton, L.A. Zenteno, "Effective area limit for large mode area laser fibers," presented at Optical Fiber Communication Conference and Exposition/National Fiber Optical Engineers Conference (OFC/NFOEC 2008), OTuJ2, San Diego, Calif., Mar. 2008.
- [7] A. Galvanauskas, M. C. Swan, and C. Liu, "Effectively single-mode large core passive and active fibers with chirally coupled-core structures," presented at Conference on Lasers and Electro-Optics/Quantum Electronics and Laser Science Conference (CLEO/QELS 2008), CMB1, San Jose, Calif., May 2008.
- [8] E. Coscelli, F. Poli, D. Passaro, A. Cucinotta, S. Selleri, T. T. Alkeskjold, L. Leick, and J. Broeng, "Single-mode regime of large mode area double cladding photonic crystal fibers," presented at European Conference on Lasers and Electro-Optics (CLEO/Europe 2011), CJ\_P20, Munich, Germany, May 2011.
- [9] F. Poli, E. Coscelli, T. T. Alkeskjold, D. Passaro, A. Cucinotta, L. Leick, J. Broeng, and S. Selleri, "Cut-off analysis of 19-cell Yb-doped double-cladding rod-type photonic crystal fibers," *Opt. Express*, vol. 19, no. 10, pp. 9896-9907, May 2011.
- [10] M. Takahashi, K. Mukasa, K. Imamura, and T. Yagi, "Single-mode holey fibers with record  $A_{eff}$  of  $50,000 \mu m^2$ ," presented at 35th European Conference on Optical Communication (ECOC 2009), Paper 7.1.1, Vienna, Austria, Sept. 2009.
- [11] M.D. Nielsen, J.R. Folkenberg, and N.A. Mortensen, "Singlemode photonic crystal fibre with effective area of  $600 \mu m^2$  and low bending loss," *Electron. Lett.*, vol. 39, no. 25, pp. 1802-1803, Dec. 2003.
- [12] W.S. Wong, X. Peng, J.M. McLaughlin, and L. Dong, "Breaking the limit of maximum effective area for robust single-mode propagation in optical fibers," *Opt. Lett.*, vol. 30, no. 21, pp. 2855-2857, Nov. 2005.
- [13] L. Dong, J. Li, and X. Peng, "Bend-resistant fundamental mode operation in ytterbium-doped leakage channel fibers with effective areas up to  $3160 \mu m^2$ ," *Opt. Express*, vol. 14, no. 24, pp. 11512-11519, Nov. 2006.
- [14] X. Peng and L. Dong, "Fundamental-mode operation in polarization-maintaining ytterbium-doped fiber with an effective area of  $1400 \mu m^2$ ," *Opt. Lett.*, vol. 32, no. 4, pp. 358-360, Feb. 2007.
- [15] L. Dong, X. Peng, and J. Li, "Leakage channel optical fibers with large effective area," *J. Opt. Soc. Am. B*, vol. 24, no. 8, pp. 1689-1697, Aug. 2007.
- [16] L. Dong, J. Li, H. McKay, A. Marcinkevicius, B. Thomas, M. Moore, L. Fu, and M.E. Fermann, "Robust and practical optical fibers for single mode operation with core diameters up to  $170 \mu m$ " presented at Conference on Lasers and Electro-Optics and Quantum Electronics and Laser Science Conference 2008 (CLEO/QELS 2008), San Jose, Calif., May 2008.
- [17] T. Wu, L. Dong, and H. Winful, "Bend performance of leakage channel fibers," *Opt. Express*, vol. 16, no. 6, pp. 4278-4285, Mar. 2008.
- [18] K. Saitoh, Y. Tsuchida, L. Rosa, M. Koshiba, F. Poli, A. Cucinotta, S. Selleri, M. Pal, M. Paul, D. Ghosh, and S. Bhadra, "Design of all-solid leakage channel fibers with large mode area and low bending loss," *Opt. Express*, vol. 17, no. 6, pp. 4913-4919, Mar. 2009.
- [19] J.M. Fini, "Bend-resistant design of conventional and microstructure fibers with very large mode area," *Opt. Express*, vol. 14, no. 1, pp. 69-81, Jan. 2006.
- [20] K. Saitoh and M. Koshiba, "Full-vectorial imaginary-distance beam propagation method based on a finite element scheme: application to photonic crystal fibers," *IEEE J. Quantum Electron.*, vol. 38, no. 7, pp. 927-933, July 2002.
- [21] K. Kakiyama, N. Kono, K. Saitoh, and M. Koshiba, "Full-vectorial finite element method in a cylindrical coordinate system for loss analysis of photonic wire bends," *Opt. Express*, vol. 14, no. 23, pp. 11128-11141, Nov. 2006.
- [22] J. Olszewski, M. Szpulak, and W. Urbańczyk, "Effect of coupling between fundamental and cladding modes on bending losses in photonic crystal fibers," *Opt. Express*, vol. 13, no. 16, pp. 6015-6022, Aug. 2005.

**Kunimasa Saitoh** (S'00-M'01) was born in Hokkaido, Japan, on July 30, 1973. He received the B.S., M.S., and Ph.D. degrees in electronic engineering from Hokkaido University, Sapporo, Japan, in 1997, 1999, and 2001, respectively.

From 1999 to 2001, he was a Research Fellow of the Japan Society for the Promotion of Science. From 2001 to 2005, he was a Research Associate of Graduate School of Engineering at Hokkaido University. In 2005, he became an Associate Professor at Graduate School of Information Science and Technology, Hokkaido University. He has been engaged in research on fiber optics, nano-photonics, integrated optical devices, and computer-aided design and modeling of guided-wave devices using finite element method, beam propagation method, and so on. He is an author or co-author of more than 100 research papers in refereed international journals.

Prof. Saitoh is a member of the Institute of Electrical and Electronics Engineers (IEEE), the Optical Society of America (OSA), and the Institute of Electronics, Information and Communication Engineers (IEICE). In 1999 and 2002, he was awarded the Excellent Paper Award and the Young Scientist Award from the IEICE, respectively, and in 2008, the Young Scientists' Prize of the Commendation for Science and Technology from the Ministry of Education, Culture, Sports, Science, and Technology (MEXT), Government of Japan. From 2009 to 2010, he served as a Secretary/Treasurer of the IEEE Sapporo Section.

**Shailendra Varshney**, biography not available at the time of submission.

**Kaori Sasaki**, biography not available at the time of submission.

**Lorenzo Rosa** received the Laurea degree in electronics engineering in 2003, and the Ph.D. degree in information technology in 2007, both from the University of Parma, Parma, Italy. From October 2007 to April 2010, he worked as a GCOE Postdoctoral Fellow at the Division of Media and Network Technologies, Graduate School of Information Science and Technology, Hokkaido University, Sapporo, Japan. Since April 2010, he has been working as a Postdoctoral Fellow in the Applied Plasmonics group of the Centre for Micro-Photonics, Swinburne University of Technology, Melbourne, Australia. His research interests include photonic-crystal fibers and waveguides, integrated optics components, finite-element and finite-difference methods for electromagnetics, integrated plasmonics, nanoantennas, photo-catalysis, and solar energy harvesting. He is a member of the Institute of Electrical and Electronics Engineers (IEEE), the Australian Optical Society (AOS), and the Optical Society of America (OSA).

**Mrinmay Pal**, biography not available at the time of submission.

**Mukul Paul**, biography not available at the time of submission.

**Debashri Ghosh**, biography not available at the time of submission.

**Shyamal Bhadra**, biography not available at the time of submission.

**Masanori Koshiba** (M'76-SM'87-F'03) was born in Sapporo, Japan. He received the B.S., M.S., and Ph.D. degrees in electronic engineering from Hokkaido University, Sapporo, Japan, in 1971, 1973, and 1976, respectively.

From 1979 to 1987, he was an Associate Professor of Electronic Engineering at Hokkaido University, and in 1987, he became a Professor there. He has been engaged in research on wave electronics, including microwaves, millimeter-waves, lightwaves, surface acoustic waves (SAW), magnetostatic waves (MSW), and electron waves, and computer-aided design and modeling of guided-wave devices using finite element method, boundary element method, beam propagation method, and so on. He is an author or co-author of more than 320 research papers in English and of more than 130 research papers in Japanese both in refereed journals. He is an author of books *Optical Waveguide Analysis* (New York: McGraw-Hill, 1992) and *Optical Waveguide*



Theory by the Finite Element Method (Tokyo, Japan: KTK Scientific/Dordrecht, The Netherlands: Kluwer Academic, 1992), and is a co-author of the books Analysis Methods for Electromagnetic Wave Problems (Boston, MA: Artech House, 1990), Analysis Methods for Electromagnetic Wave Problems, Vol. Two (Boston, MA: Artech House, 1996), Ultrafast and Ultra-parallel Optoelectronics (Chichester, UK: Wiley, 1995), and Finite Element Software for Microwave Engineering (New York: Wiley, 1996).

Prof. Koshihara is a fellow of the Institute of Electrical and Electronics Engineers (IEEE), the Optical Society of America (OSA), and the Institute of Electronics, Information and Communication Engineers (IEICE), and is a member of the Institute of Electrical Engineers of Japan and the Institute of Image Information and Television Engineers of Japan. In 1987, 1997, and 1999, he was awarded the Excellent Paper Awards from the IEICE, in 1998, the Electronics Award from the IEICE-Electronics Society, and in 2004, the Achievement Award from the IEICE. From 1999 to 2000, he served as a President of the IEICE-Electronics Society, and in 2002, he served as a Chair of the IEEE-LEOS (Lasers and Electro-Optics Society) Japan Chapter. From 2003 to 2005, he served on the Board of Directors of the IEICE. In 2008, he serves as a Chair of the IEICE Hokkaido Chapter, and from 2009, he serves as a Chair of the IEEE Sapporo Section.